

Maximizing Contact of Supersoft Bottlebrush Networks with Rough Surfaces To Promote Particulate Removal

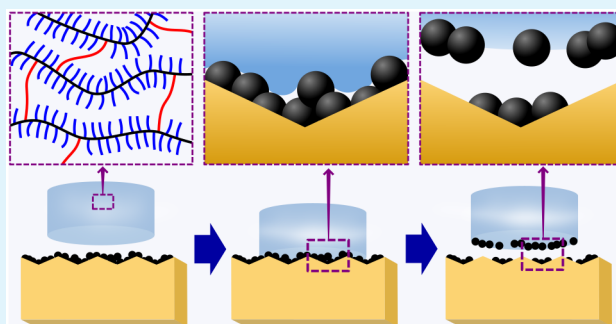
Teresa T. Duncan,¹ Edwin P. Chan,^{1*} and Kathryn L. Beers

Material Measurement Laboratory, National Institute of Standards and Technology, Gaithersburg, Maryland 20899, United States

Supporting Information

ABSTRACT: Efficient removal of particulates from a rough surface with a soft material through a “press and peel” method (i.e., an adhesion and release approach) depends on good conformal contact at the interface; a material should be sufficiently soft to maximize contact with a particle while also conforming to rough surface features to clean the entire substrate surface. Here, we investigate the use of bottlebrush networks—extremely soft elastomers composed of macromolecules with polymeric side chains—as materials for cleaning model substrates of varying roughness. Formed through free-radical polymerization of mono- and dimethacrylate functionalized polysiloxanes, these solvent-free supersoft elastomers exhibit moduli comparable to those of solvated gels, allowing for a lower moduli regime of elastomers to be used in contact experiments than previously possible. By varying the macromonomer to cross-linker ratio, we study the effect of modulus on conformal contact and cleaning for materials that are as soft as gels while minimizing/negating physical and/or chemical concerns that using a traditional material may involve (e.g., changes in component concentrations, solvent evaporation, and syneresis). We study cleaning efficacy by quantifying the conformal contact between soft materials and rough substrates via a contact adhesion-based measurement. These results give insight into the correlation between shear modulus and conformal contact with surfaces of varying feature height. Not only does a decrease in shear modulus leads to improved conformal contact with rough surfaces, but also it facilitates adhesion to particulates situated on the rough surface, thus aiding removal. We highlight this property control with a case study illustrating the removal of an artificial soil mixture from a rough, acrylic surface via peeling rather than rubbing, which can cause damage to delicate surfaces.

KEYWORDS: bottlebrush polymers, elastomers, conformal contact, cleaning, cultural heritage



1. INTRODUCTION

The ability of a material to make intimate contact with a surface depends on the roughness and deformability of the interface. Complete conformal contact is a challenge in cases where both the components are rigid and at least one of them is rough. The degree of conformal contact can be improved by increasing the softness of one or both components. For this reason, soft materials have been applied to a range of technologies that require intimate contact between two surfaces, including soft lithography,^{1,2} drug delivery,³ wearable electronics,⁴ imaging,^{5,6} adhesives,^{7–9} and art conservation.^{10–12}

In the context of conservation of works of art, soft materials (i.e., gels) have been used in a variety of applications, including material (e.g., pigment) identification,^{13–15} solvent delivery to aid in the removal of stains or deteriorated layers,^{16–18} or removal of particulate contaminants.^{19–22} One common feature in all of these applications is the requirement for a gel to make intimate contact with a substrate surface. Although the removal of contaminants from delicate surfaces can be achieved with dry (e.g., laser ablation,^{23,24} microfiber cloths,²⁵ and polymeric micropillars²⁶) and wet (e.g., solvents,

surfactants,²⁷ and microemulsions²⁸) methods, gels have been shown to be a gentle and effective strategy.^{22,29,30} However, the contact between soft cleaning materials (e.g., gels) and substrates has not been investigated in relation to cleaning efficacy.

The contact efficiency of a gel with a substrate can be described broadly by the Dahlquist criterion.³¹ This criterion states that the elastic modulus (E) of a material must be below 0.1 MPa for contact to occur between a deformable or “soft” solid with a rigid or “hard” substrate.³¹ However, the Dahlquist criterion does not account for variations in surface roughness. Surface roughness, elastic modulus, contact time, magnification (i.e., length scale of observation), and contact pressure have all been shown to affect the contact area and adhesion that result when a “soft” solid is pressed to a “hard”, rough substrate.^{32–37} Those materials considered “soft” have a wide range of E , with experiments probing materials with E as low as 1 MPa.^{38,39} Weakly cross-linked polymer gels of lower elasticity—with E

Received: September 27, 2019

Accepted: November 12, 2019

Published: November 12, 2019

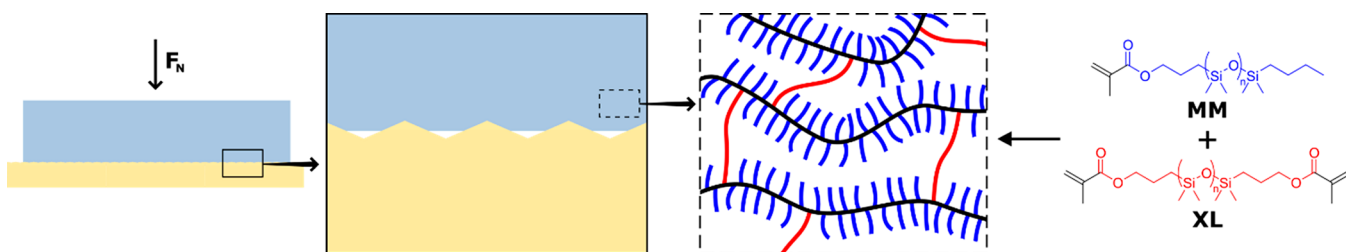


Figure 1. When an elastic or viscoelastic solid is pressed into contact with a rigid substrate of some degree of roughness, the true and apparent contact areas may differ (solid inset). The effect of elastic modulus on the contact area between these two materials can be studied by employing a bottlebrush network (dashed inset) in a contact experiment. The cross-linking density of the network can be altered by varying the ratio of side chains (blue) to cross-linkers (red), thereby producing a series of materials of varying moduli.

typically ranging from 1 to 500 kPa—have fallen outside the scope of these studies, presumably due to the significant complications that a liquid additive may add in the contact between a gel and a substrate.

Bottlebrush networks (BBNs), which are composed of densely grafted polymeric side chains extending from a cross-linked polymeric network, have been demonstrated as “supersoft” materials with moduli comparable to polymer gels but without any liquid additives.^{40,41} More importantly, changes to the BBN architecture (i.e., the molecular masses of components and/or cross-linking density) allow for precise control over (1) the modulus and (2) the stress–strain behavior without significant changes to the chemistry.^{42,43} In this study, we make advantageous use of BBNs as model “supersoft” materials to study conformal contact as a function of modulus (Figure 1). We present a simple method to image and quantify conformal contact with model rough substrates, and we show soft materials can make good conformal contact with rough substrates of large feature height ($\approx 55 \mu\text{m}$) that scales with the modulus of the material. Finally, we demonstrate that this high degree of conformal contact can enhance particulate removal from rough surfaces.

2. EXPERIMENTAL SECTION

2.1. Materials. Macromonomer, MM (monomethacryloxypropyl-terminated polydimethylsiloxane (PDMS), Gelest, MCR-M11, $M_n = 980 \text{ g/mol}$ from ^1H NMR, Table S1), and cross-linker, XL (methacryloxypropyl-terminated PDMS, Gelest, DMS-R22, $M_n = 8800 \text{ g/mol}$ from ^1H NMR, Table S1), were passed through a short alumina plug before use with dichloromethane (Fisher Scientific, ACS grade) as the eluent. Toluene (Taylor Scientific, ACS grade), acetone (Fisher Scientific, ACS grade), hexanes (J. T. Baker, >95%), ethanol (Warner Graham Co., 200 proof), BAPOs (phenylbis(2,4,6-trimethylbenzoyl)phosphine oxide, >96%, TCI America), Sylgard 184 PDMS (Dow Corning), and Norland optical adhesive 60 were used as received.

2.2. Preparation of Bottlebrush Networks. 0.90 g of methacrylate-functionalized PDMS (i.e., macromonomer MM and cross-linker XL in the appropriate molar ratio) was added to a vial along with 0.58 g of toluene. All samples were sparged with argon for 10 min. In an argon-filled glovebox, BAPOs (5 mol % relative to methacrylate functionalities on MM and XL) was added to each vial. The solutions were stirred for 2 min and transferred with a pipet to a Teflon mold. The solutions were irradiated under an ultraviolet (UV) lamp (365 nm, 0.1 mW/cm²) for 18 h, transferred from the mold to a preweighed glass slide, vacuum-dried at 40 °C overnight, and weighed. Samples on glass slides were transferred to screw top-sealed jars, washed with three aliquots of acetone (selected as the solvent due to its ability to dissolve starting materials without causing significant swelling of the BBN) over 3 days, and vacuum-dried at 40 °C overnight. Each sample was weighed again to determine gel fraction.

2.3. Preparation of Sylgard 184. A 20 to 1 or 10 to 1 ratio by mass of base to curing agent mixture was stirred vigorously for 3 min and poured into a Petri dish. After resting 1 h (until bubble-free), the mixture was heated at 65 °C for 2 h under atmospheric pressure. Samples were washed with three aliquots of hexanes over 3 days.

2.4. Mechanical Measurements. The shear modulus (G) of each prepared material was quantified by using a contact adhesion testing (CAT) instrument.⁴⁴ A spherical glass probe, of radius $r = 1 \text{ mm}$, was brought into contact with the sample at a crosshead speed of $5 \mu\text{m/s}$ up to a compressive load of 0.2 g. Optical images—obtained with a Leica DMIRE2 inverted microscope coupled to a JAI BM-500GE camera—were collected during the contact experiment to measure the contact radius (a) at applied displacement (δ) and corresponding load (P) values. A correction factor for P was used to account for the influence of substrate stiffness: for the geometric confinement regime $a/t < 0.5$ (as tabulated in Table S2) and materials of sample thickness t , $P' = P(1 - a/t)$.⁴⁵ By assuming the materials are isotropic and incompressible (Poisson’s ratio $\nu = 0.5$), G was extrapolated from the slope of an effective stress, P'/a^2 , versus effective strain, $2\left(\frac{\delta}{a} + \frac{a}{3R}\right)$, curve via

$$\text{slope} = \frac{E}{1 - \nu^2} = \frac{2G}{1 - \nu} \quad (1)$$

2.5. Preparation of Model Rough Substrates. An S-22 microfinish comparator (Gar Electroforming Div.) was placed in an aluminum foil tray (Figure S1), and a 20 to 1 ratio by mass of base to curing agent of Sylgard 184 was stirred vigorously for 3 min and poured onto the surface of the comparator. A microfinish comparator is an electroformed surface roughness scale created to replicate machined surfaces. After resting for 1 h (until bubble-free), the Sylgard-coated comparator was heated at 75 °C for 2 h under atmospheric pressure. After cooling to room temperature, the cured Sylgard was peeled from the surface of the microfinish comparator. A razor blade was used to cut 1 cm \times 1 cm sections from three patterns: 63ST, 250ST, and 500ST, replicas of shape-turned machined surfaces with grooved patterns of different roughnesses. Norland optical adhesive—sandwiched between patterned and smooth Sylgard sections with 1 mm Sylgard spacers—was UV-cured (365 nm, 0.1 mW/cm²) overnight to result in a 0.5 cm \times 0.7 cm Norland copy of the microcomparator surface. These Norland copies were taped—rough side facing down—to a glass slide, and a 2.5 mm \times 2.5 mm section was cut with a CO₂ laser cutter (Full Spectrum Laser Hobby). The resulting squares were sonicated in ethanol 10 min, the adhesive tape was removed, and a drop of Norland optical adhesive was used to affix each of the squares—rough side facing up—to a glass slide with UV curing (365 nm, 0.1 mW/cm²) for 1 h. The surface profiles of the rough substrates were measured with an optical profilometer (Zygo NewView 7300).

2.6. Conformal Contact Measurements. The conformal contact was measured with the CAT instrument. Specifically, the glass spherical probe was replaced with a model rough substrate, and the contact with a soft material was imaged by using a camera connected to the inverted microscope. Each soft material (ranging in thickness from 2.6 to 3.2 mm) was aligned using the tilt stage of the

CAT instrument and brought into contact with each rough surface at a fixed displacement rate (crosshead speed = 5 $\mu\text{m/s}$) up to a compressive load of 9 g, a magnitude similar to what one may use if they gently press a finger onto a substrate. Upon reaching the maximum compressive load, the sample was held in contact with the rough substrate for 30 s (to allow for the contact area to remain unchanged with time), at which point the sample was retracted at a crosshead speed of 5 $\mu\text{m/s}$. This contact experiment was performed for the three substrates of varying feature height in contact with five elastomers of varying G : a 10:1 ratio by mass of base to curing agent Sylgard sample ($G = 352$ kPa); a 20:1 ratio by mass of base to curing agent Sylgard sample ($G = 126$ kPa); a 0:1 molar ratio of MM to XL sample ($G = 114$ kPa); a 10:1 molar ratio of MM to XL BBN sample ($G = 21$ kPa); and a 50:1 molar ratio of MM to XL BBN sample ($G = 1$ kPa). Optical images collected throughout the experiment were used to estimate conformal contact. By applying an edge detection image processing protocol to the optical images obtained, certain pixels can be mapped as “edges”, which are pixels that are designated as high contrast. ImageJ⁴⁶ and a “Canny Edge Detector”⁴⁷ plug-in were employed to map “edges” with a Gaussian kernel radius of 0.5, a low threshold of 4.5, and a high threshold of 5.5. We estimate conformal contact (C_c) as the percent loss of pixels defined as edges

$$C_c (\%) = \left(1 - \frac{e_d}{e_b}\right) \times 100\% \quad (2)$$

where e_b and e_d represent the percentage of pixels defined as edges before and during contact, respectively.

2.7. Cleaning Experiments. We used the CO₂ laser cutter to cut and pattern a 7.6 cm \times 2.5 cm section of an acrylic sheet (Optix Plaskolite) with a series of shallow, parallel lines (3 mm apart; 1% power). A hydrophobic artificial soil mixture was prepared by using a literature formulation⁴⁸ by combining kaolin (1.0 g, Fisher Scientific Laboratory grade), soluble starch (0.5 g, Mallinckrodt), gelatin (0.5 g, Sigma-Aldrich Type B from bovine skin), iron oxide (0.025, raw sienna, Conservation Materials, Ltd.), lamp black (0.1 g, Conservation Materials, Ltd.), silica (0.088 g, Fisher, special fine granular, 80 to 120 mesh), concrete (0.88 g, Sakrete Portland Cement Type I-II), mineral oil (1 mL, Fisher Scientific, light), and olive oil (0.5 mL, Crisco pure olive oil). 20 mg of artificial soil was suspended in 1 mL of hexanes, and \sim 0.5 mL of the mixture was transferred to the plexiglass surface with a glass pipet. This resulted in the formation of a layer of artificial soil deposited onto the acrylic surface following evaporation of the solvent under ambient conditions. Gravimetric measurement of the patterned plexiglass substrate before and after soil deposition showed the artificial soil surface coverage to be \sim 0.4 mg/cm². The topography of the patterned acrylic was imaged before and after soil deposition with an optical profilometer.

Cleaning experiments were conducted using the CAT instrument. Specifically, the soil-coated, patterned substrate was mounted onto the glass substrate holder. A 3 mm diameter cylinder of the soft material, cut with a 3 mm biopsy punch, was aligned by bringing it into contact with a clean portion of the acrylic surface and by using the tilt stage of the CAT instrument to ensure uniform contact. The cylinder of soft material was then brought into contact with the soil-coated, rough surface at a crosshead speed of 5 $\mu\text{m/s}$ up to a load of 7.1 g. The contact was allowed to dwell for 30 s, at which point the sample was retracted at a crosshead speed of 5 $\mu\text{m/s}$. It should be noted that we use a normal pull off geometry rather than a peeling retraction geometry: conservators may use either geometry for a cleaning treatment, depending on the properties of their selected cleaning material and substrate. Optical images of the rough surfaces were collected throughout the contact experiment, and the images taken before and after contact were subtracted and thresholded with ImageJ.

3. RESULTS AND DISCUSSION

3.1. Characterization of BBNs. Clear, solvent-free BBN elastomers were produced through the photopolymerization of

methacrylate-functionalized macromonomer (MM) in the presence of cross-linker (XL), as illustrated by the chemical structures in Figure 1. The cross-linking density of the BBN elastomers was systematically controlled by varying the molar ratio of macromonomer to cross-linker (MM:XL). Gel fractions, defined as the percent by mass of MM and XL that are incorporated into the network, ranged from 73% to 99% (Table 1). The shear modulus G of each BBN was

Table 1. Gel Fractions and Shear Moduli (G) of BBN Elastomers as a Function of Molar Ratio of MM to XL

molar ratio of MM to XL	batch	gel fraction (mass %)	$G^{a,b}$ (kPa)
0:1	1	93	219 \pm 7
	2	99	114 \pm 22
	3	87	116 \pm 31
10:1	1	79	58 \pm 16
	2	87	21 \pm 1
	3	75	13 \pm 3
30:1	1	73	15 \pm 0.3
	2	74	2.1 \pm 0.5
	3	73	1.1 \pm 0.2
50:1	1	68	3.0 \pm 0.5
	2	74	1.3 \pm 0.3
	3	72	1.1 \pm 0.3

^aAs determined from contact adhesion testing. ^bAverage value from three trials on one sample with associated standard deviation.

determined by using CAT (Figure 2), and the values are in good agreement with the values obtained from oscillatory shear rheology (Figure S2 and Table S3). As shown in Table 1, G increases with increasing cross-linking density, which is consistent with previous results of BBN elastomers.^{40,43} More importantly, we can vary G over more than 2 orders

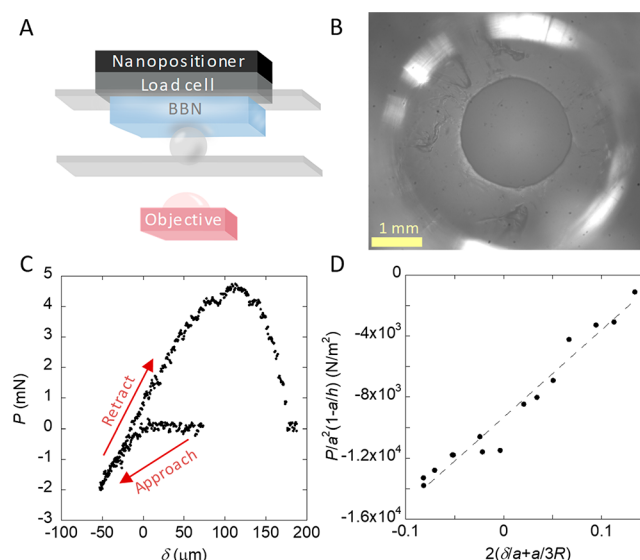


Figure 2. Representative contact adhesion test (CAT) experiment. The CAT experiment involves bringing a glass sphere into contact with the soft elastomer (A). The contact area (πa^2) at the interface (B) as well as the force P and displacement δ are measured (C) during the entire test. The slope of $P/a^2(1 - a/h)$ versus $2(\delta/a + a/3R)$ (D) for data collected during the “approach” portion of the experiment can be used to determine G .

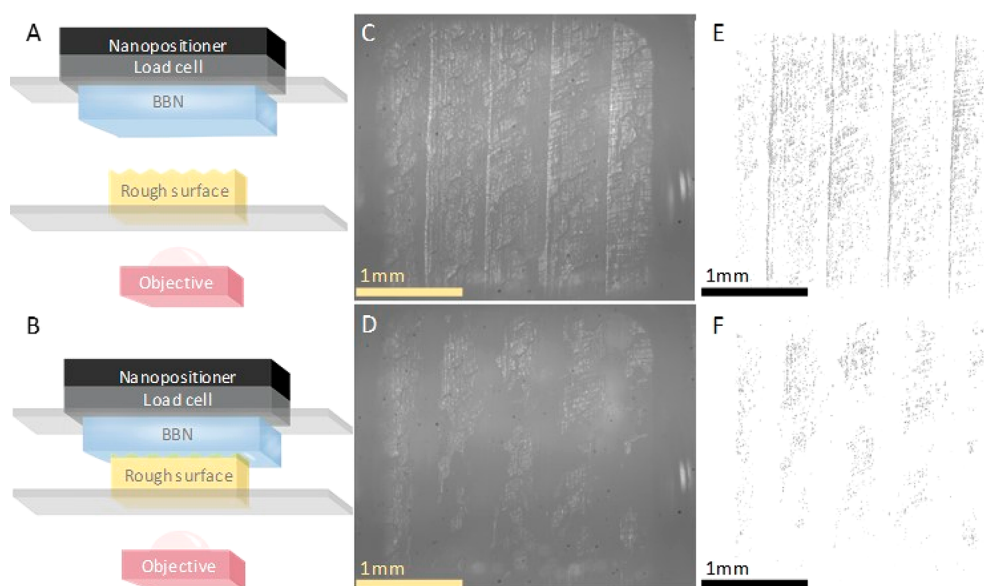


Figure 3. In a conformal contact experiment, a bottlebrush network (BBN) or other elastomer is mounted to a glass slide attached to a load cell and nanopositioner (A). It is brought into contact with a rough substrate surface (B). Images collected of rough surface with feature height of $30\ \mu\text{m}$ before (C) and during (D) contact with BBN of $G = 21\ \text{kPa}$ show a loss of contrast in areas where contact occurs. A “Canny edge detect” protocol applied to the images before (E) and during (F) contact map high contrast pixels as black, and these edge maps can be used to estimate the percent conformal contact.

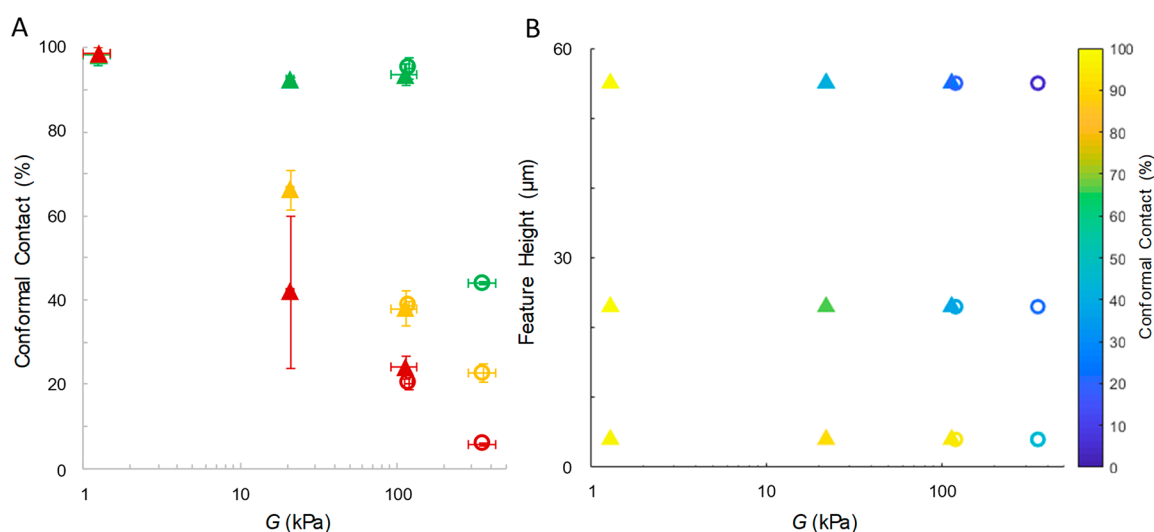


Figure 4. Characterizing conformal contact between soft elastomers and substrates of three different roughnesses. Percent conformal contact versus G (A) of the various soft elastomers including BBN (closed triangles) and Sylgard 184 (open circles) samples. The three substrates consist of feature heights of $4\ \mu\text{m}$ (green), $23\ \mu\text{m}$ (yellow), and $55\ \mu\text{m}$ (red). The maximum load per area applied to each sample was $13\ \text{mN}/\text{mm}^2$. Error bars designate the standard deviation from three trials of three different contact locations on the same sample. Contact map (B) of the same data set, but with color used to designate percent conformal contact as displayed in the colorbar.

of magnitude, which is quite challenging for traditional elastomers by changing only the ratios of starting materials.

3.2. Conformal Contact of Soft Elastomers with Rigid, Rough Surfaces. We conducted conformal contact experiments to quantify the degree of conformal contact between the soft elastomers and rough surfaces. For these experiments, we modified the CAT instrument by replacing the glass sphere used in our characterization studies with model rough substrates (Figure 3A,B) and then brought these surfaces into contact with the soft elastomers. To produce model rough substrates, replicas of different linear patterns from a microfinish comparator were cast in Norland optical adhesive and laser cut to approximately $2.5\ \text{mm} \times 2.5\ \text{mm}$ (a sufficiently

small dimension so that the entire substrate was imaged during contact experiments). Optical microscopy and profilometry were used to collect topographical information about the prepared rough surfaces (Figure S3 and Table S4). Surface profiles indicated that the peak-to-valley heights for the three surfaces were 10 , 31 , and $59\ \mu\text{m}$ with respective feature heights (i.e., the depth of each v-notch) of 4 , 23 , and $55\ \mu\text{m}$ (with standard deviations in height of $1\ \mu\text{m}$ or less). The deviation between the peak-to-valley heights and the feature heights indicates there is a slight curvature to the substrate.

Figure 3 shows a representative conformal contact experiment between a soft elastomer and a model rough substrate. Comparing Figure 3C (prior to contact) with Figure 3D (in

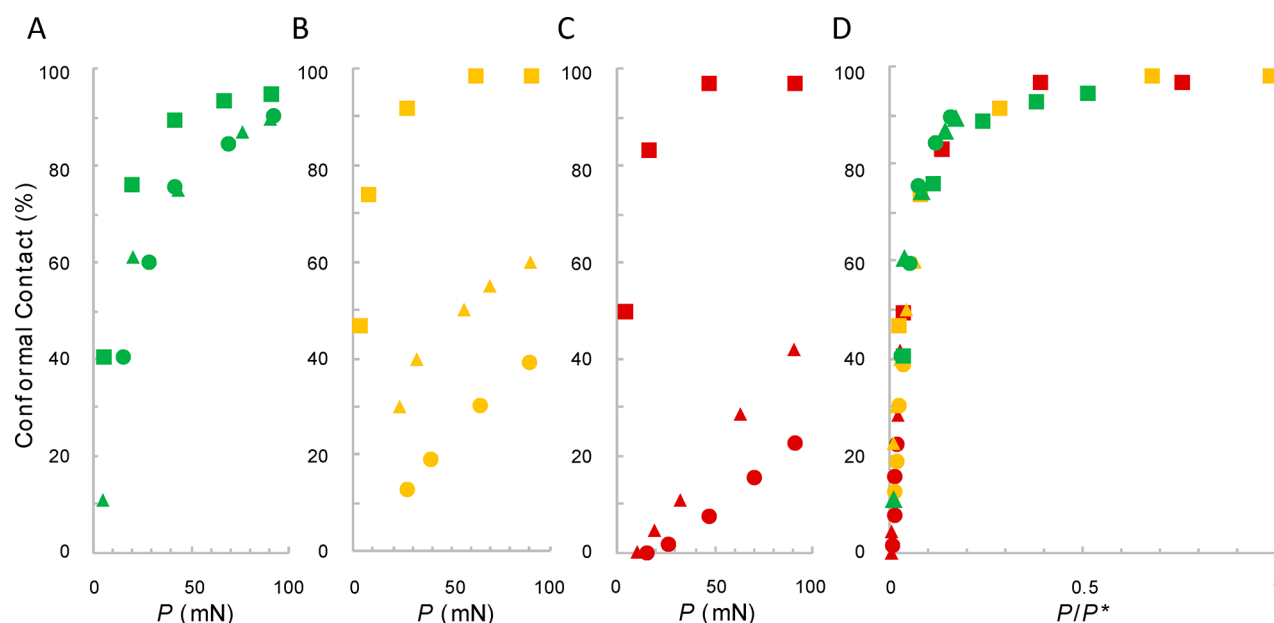


Figure 5. Conformal contact versus applied load. Percent conformal contact for BBNs of varying G (circles = 114 kPa, triangles = 21 kPa, and squares = 1 kPa) in contact with rough substrates with feature heights of 4 μm (A), 23 μm (B), and 55 μm (C). Conformal contact versus normalized load (P/P^*) for all rough surfaces with features heights of 4, 23, and 55 μm represented by green, yellow, and red, respectively (D). P^* is the estimated critical load required to reach complete conformal contact.

contact), we see that there is a loss of contrast in the areas of the rough surface where it is in contact with the soft elastomer. The edge maps (which designate high contrast pixels as black) of images collected before (Figure 3E) and during (Figure 3F) contact correlate well with the raw images. The images and edge maps of contact experiments with the three rough surfaces and a range of elastomers of varying G are displayed in Figures S4–S8.

The percent change in the number of high contrast pixels upon contact is used as a measure of the extent of conformal contact between the soft elastomers and model rough substrates. A plot of percent conformal contact versus G of the soft elastomers (Figure 4A) shows that conformal contact increases with (1) decreasing G and (2) decreasing feature height. The BBN elastomer composed of a 50:1 of MM to XL was sufficiently soft to make good contact with all three rough surfaces. There appears to be a critical G for each rough surface above which contact begins to decrease drastically due to the elastomer's resistance to deformation over the entire feature. We replot the data in Figure 4A as a contact map (Figure 4B) to use it as a design map for identifying an elastomer with the appropriate properties that provides the required contact with surface topography of a given size scale.

Figure 5A–C summarizes the increase in conformal contact between the soft elastomers and the model rough substrates as a function of applied load. We find that contact increases with applied load in all cases. Although this trend is true irrespective of the specific model rough substrate and elasticity of the soft elastomer, the magnitude of increase in contact decreases with increasing surface roughness and modulus.

The relationship between conformal contact, intrinsic mechanical properties, and applied pressure has been previously studied by several groups.^{34,36,37,49} At small applied pressures (i.e., when the applied pressure is smaller than the interfacial forces), Creton and Liebler³⁴ suggested that contact can be described by the theory of Johnson, Kendall, and

Roberts (JKR). Conformal contact (C_C) will occur even in the absence of applied pressure so that contact scales with G

$$C_C \sim \left(\frac{G_0 R^2}{3G} \right)^{2/3} \quad (3)$$

where G_0 is the thermodynamic work of adhesion and R is the radius of curvature of asperities on a randomly rough surface. At “large pressures” (i.e., where the applied pressure exceeds the interfacial forces), Creton and Liebler suggested that contact can be described by Hertz contact mechanics such that the relationship between C_C and P scale with G as

$$C_C \sim \frac{P}{3G} \left(\frac{R}{\sigma} \right)^{1/2} \quad (4)$$

where the ratio R/σ is related to the substrate roughness with σ denoting the standard deviation of the height distribution of the asperity. Equation 4 suggests that when a soft material makes contact with a surface with a characteristic roughness R , the degree of conformal contact should increase linearly with P . Although this trend is consistent with our results at contact below 40%, we see a deviation from linearity at higher contact where a greater amount of force must be applied to the elastomer to increase conformal contact with the rough surface.

Johnson and co-workers⁵⁰ presented a closed form solution to a similar problem where a soft 2D periodically rough material is brought into complete contact with a rigid substrate. Using a fracture mechanics approach, they showed the relationship between contact and P has an asymptotic solution and that a critical pressure (P^*) must be applied to establish 100% conformal contact. This critical pressure $P^* \approx Gf(\epsilon)$ where $f(\epsilon)$ is the nonlinear strain function, which accounts for the hyperelastic deformation behavior of soft elastomers. We applied this scaling approach to our results and found that by normalizing the applied pressure by an

approximate critical pressure P^* (the values of which are tabulated in Table 2 and which we estimated by approximating

Table 2. P^* Values (in mN/m^2) Used in the Normalization of P (Figure S5)

G (kPa)	feature height of rough surface		
	4 μm	23 μm	55 μm
114	85	400	800
21	75	190	460
1	25	13	17

at what pressure 100% contact would occur), the contact curves can be shifted to fit onto a single curve (Figure S5). These master curves highlight how the increase in contact is linear at low degrees of contact, but the slope decreases as contact increases and approaches the maximum possible contact of 100%.

3.3. Conformal Contact of Soft Hydrogels with Rough Surfaces. As a comparison, we also conducted conformal contact experiments using agarose and gellan hydrogels, which are materials commonly used in the conservation of art.^{10,11,51}

When we compare Figure 4 with Figure S11, we find that both the agarose ($G = 41$ kPa) and gellan ($G = 48$ kPa) hydrogels made more efficient contact (Figures S9–S11), ranging from 86% to 100% for all three rough substrates, compared with elastomers of similar modulus. We ascribe this increase in conformal contact to several subtle but distinct chemical and physical differences between the elastomers and the hydrogels. (1) Although both the BBN elastomers and hydrogels undergo viscoelastic relaxation when deformed against a rough surface, the hydrogels display another form of stress relaxation associated with poroelasticity, which is related to solvent diffusion due to an imposed stress.⁵² (2) The BBN and PDMS elastomers are chemically cross-linked networks with significantly higher fracture toughness than the physically cross-linked hydrogels. Upon release of the soft material from the rough surface, the hydrogel surfaces were observed to have been imprinted with the rough surface topographies and the elastomers were not, thus suggesting that the hydrogels were permanently deformed during the conformal contact experiments. This deformation is probably caused by the reorganization or fracture of physical cross-links of the hydrogel when brought into contact with the rough surface. The difference in the relaxation behavior of the soft networks can be noted during the dwell portion of the contact experiment (when the maximum displacement is held constant for 30 s): the load response of the BBN is unchanged over 30 s, but the load responses of the hydrogels decreases significantly

(Figure S12). The BBN acts as a soft spring, with little hysteresis at large loads, whereas the hydrogels show a significant amount of hysteresis between the approach and retraction curves.

3.4. Removal of Particulates from a Soil-Coated Surface. Works of art are susceptible to surface deposition of dust, dirt, grease from fingerprints, air pollutants, and other types of contaminants from a host of sources.⁵³ Not only can these contaminants mar the appearance of the work of art, but they can also lead to irreversible chemical degradation of the surface. Thus, art conservators must periodically clean them by either removing contaminants from the topmost layer or by removing deteriorated layers altogether.⁵⁴ Typically, gels are used to deliver a cleaning liquid to the topmost layer of the art surface. However, recent studies have demonstrated that gels can be used to gently remove particulate contaminants by pressing and peeling from the surface.^{20,21,49} For a gel to be effective in removing particulates from a surface, it should be able to (1) conform to the topography of the rough surface (to increase the surface area capable of being cleaned), (2) conform around individual particulates (as an increase in contact area will increase the adhesive force between the two materials), and (3) provide favorable surface energetics at the interface to promote chemical adhesion.

Because BBNs were shown to be capable of conforming to rough surface features, we hypothesized that BBNs could conform not only to these large-scale features but also to smaller particles that cover these large-scale features. If the adhesion energy between the BBNs and particles⁵⁵ exceeds that between the particles and substrate, we anticipated that the particles could be removed from the substrate. To test these hypotheses, a laser-engraved acrylic substrate was coated with a thin layer of an artificial soil mixture, and elastomers of varying G are pressed to and peeled from the soil-coated substrate (Figure 6). Acrylic sheet was chosen as a representative material because it is an optically clear substrate with low scratch resistance that can be found in museum settings, both as an artists' material and for display purposes.⁵⁶ We laser engraved the acrylic substrates to pattern the surfaces with topography consisting of approximate feature sizes of 50 μm deep grooves below and 10 μm ridges above the flat surface. Surface profiles of the patterned substrate before and after soil deposition are presented in Figure S13 and Table S5. Optical images of these patterned surfaces were collected before, during, and after contact with soft elastomers of $G = 352$, 114, and 1 kPa (Figure 7). Images collected during contact (Figures 7B, 7F, and 7K) highlight how only the supersoft bottlebrush elastomer (Figure 7K) was able to conform around the soil particulates and make contact with the

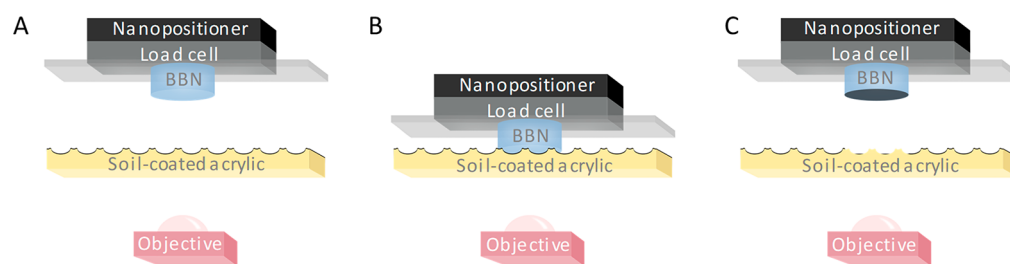


Figure 6. In a cleaning experiment, a cylindrical bottlebrush network (or other elastomer) sample—mounted to a glass slide attached to a load cell and nanopositioner (A)—is brought into contact with a soil-coated, patterned acrylic substrate (B). The sample is then raised from the substrate, resulting in transfer of some of the soil from the substrate to the sample (C).

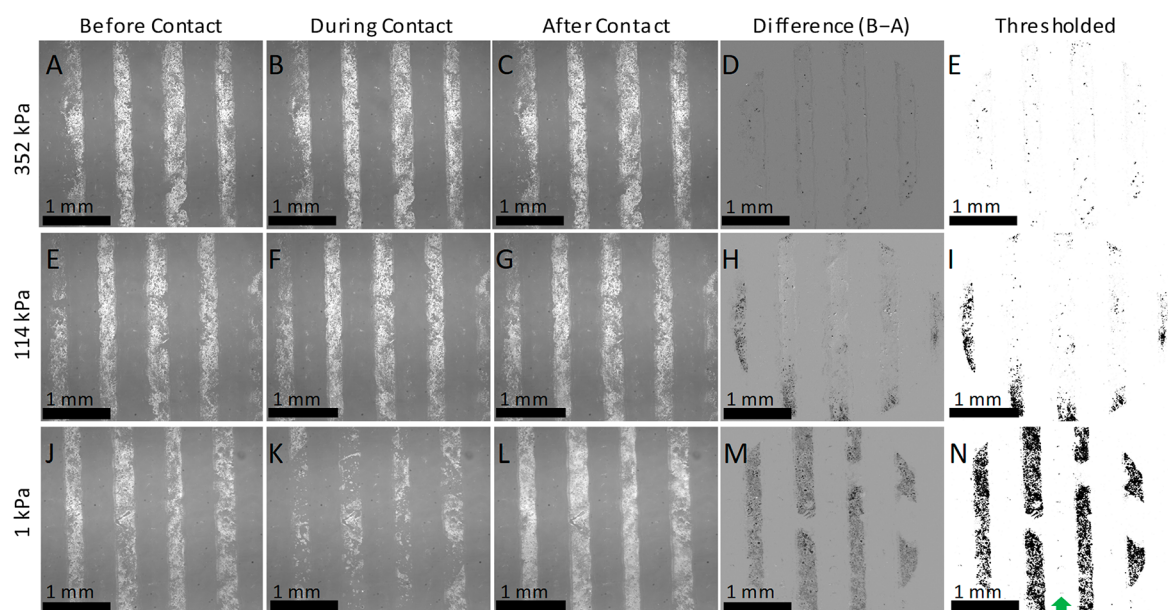


Figure 7. Optical images of soil-coated, patterned acrylic substrate before (A), during (B), and after (C) contact with a 10:1 ratio by mass of base to curing agent Sylgard 184 sample ($G = 352$ kPa); before (E), during (F), and after (G) contact with a 0:1 molar ratio of MM to XL sample ($G = 114$ kPa); and before (J), during (K), and after (L) contact with a 50:1 molar ratio of MM to XL sample ($G = 1$ kPa). Before and after images were subtracted to produce the difference images (D, H, M) which were thresholded (E, I, N) to designate areas cleaned as black and unchanged as white. Green arrow in (N) identifies a valley from which soil was removed.

substrate (resulting in a dark, circular pattern that encompasses most of the image window).

To better reveal the extent of cleaning efficacy of the soft elastomers, we use image subtraction to generate difference images. Specifically, the difference image is obtained by performing an image subtraction of the “before contact” and “after contact” images followed by thresholding the resultant image. Regions of this image consisting of black pixels are defined as cleaned, and gray pixels are defined as uncleared. Figures 7E, 7I, and 7N show the cleaning efficacy of the soft elastomers with decreasing elasticity. Not only did the total area cleaned increase with decreasing G , but also the softest elastomer (Figure 7M,N) was sufficiently compliant such that it was able to conform considerably to the topography of the patterned acrylic substrate, thus enabling contact and subsequent removal of particulates in the valleys (which is identified with the green arrow in Figure 7N). Optical images of the soft elastomers after pressing and peeling from the soil-coated substrate highlight the enhanced cleaning efficacy of the softest material: the 1 kPa BBN was evenly coated with a larger amount of soil, whereas the stiffer materials collected a smaller amount, mainly from the ridges that protrude $10\ \mu\text{m}$ from the patterned acrylic surface (Figure S14).

Gellan and agarose are both hydrogels used by art conservators, typically for solvent delivery, and here we highlight their additional ability to remove soil through a gentle, pressing and peeling method. Hydrogels formed from either agarose or gellan were used to remove soil from the soil-coated, patterned acrylic substrate (Figure S15). Although these materials appeared to make better contact with the substrate (Figure S15B,H) than the BBN of $G = 1$ kPa, their cleaning ability was not as effective. This reduction in cleaning efficacy could be attributed to lower adhesive forces between the gel and the particulates, exacerbated by the higher polarity of the gelator and lubrication effects from the water. Although these hydrogels may not be as effective as the studied

elastomers for “press and peel” removal of this particular artificial soil mixture, these results do show that certain hydrogels that are currently used by conservators can be used to remove soil particulates from a surface. By tuning the properties of hydrogels, either through changes in component concentrations or the addition of components to the gels, conservators should be able to optimize the conformal contact and cleaning efficacy for their specific substrates.

In the decision-making process to choose a certain cleaning treatment, a conservator will weigh the risk of residues that may remain on the object after treatment. For gel or elastomer residues from a cross-linked network to remain on a substrate after peeling, cohesive failure must occur. Although tuning the stiffness of soft materials is an effective method for promoting conformal contact with rough surfaces, decreasing the cross-linking density within a network often leads to a decrease in the cohesive energy of the material. In cases where the adhesion energy with a substrate surpasses the cohesive energy of the material, there is a greater propensity for the soft material to fracture, with some portion of the material remaining after its release from the substrate. In this study, cohesive failure was not noted visually upon separating the BBNs from acrylic or Norland substrates. The adhesion between a soft material and a substrate will depend on a host of factors, most notable is the chemistry of the substrate, which for a work of art will depend on the materials used by the artist and any changes that will have occurred upon aging.

4. CONCLUSION

The degree of conformal contact between soft materials and rough surfaces depends on a host of parameters, and here we show how the shear modulus of soft materials—with G ranging from 1 to 352 kPa, the lower end of which was enabled by the recent development of the BBN polymer architecture—can be tuned to promote interfacial conformal contact with rough surfaces, as imaged by adapting a typical CAT experiment. A

major advantage of the CAT instrument is the ease of adaptability to probe contact and adhesion between substrates of various topographies: similar instrumental protocols have been used to measure contact and adhesion between smooth probes and deformable, rough (e.g., patterned⁵⁷ or wrinkled⁵⁸) surfaces, but our work highlights the ease of adaptability of the probe itself. Our pattern fabrication methodology used to prepare the probe is adaptable to a wide range of soft materials and rough substrates as long as the surface pattern can be replicated via microfabrication approaches and can be imaged under an optical microscope.

Achieving good conformal contact with surfaces was shown to be critical for the removal of particulates from rough surfaces. Softer elastomers demonstrated increasing cleaning efficacy because of three important design requirements: (1) an increase in the contact area with the rough substrate surface so that the entire surface can be cleaned, not just the portions of features that protrude most from the substrate, (2) an increase in the number of contacts with particulates on the substrate surface aided by the ability of the soft materials to conform to the smaller scale roughness (in comparison to the larger scale roughness of the rough substrate) inherent to the soil coating, and (3) an increase in the size of each individual contact area between a solid particle and the soft material, as an increase in the contact area leads to an increase in the adhesion force between the soft material and the particles. These fundamental factors contribute to aid in the removal of the artificial soil particulates through a “press and peel” method, which was shown to be effective for the removal of artificial soil from surfaces with a host of soft materials, ranging from hydrogels to Sylgard 184 to BBNs.

■ ASSOCIATED CONTENT

■ Supporting Information

The Supporting Information is available free of charge at <https://pubs.acs.org/doi/10.1021/acsami.9b17602>.

Number-average molecular mass (M_n) of starting materials; schematic of preparation of model rough surfaces; strain and frequency sweeps of BBNs, optical images and surface topographies of model rough surfaces; optical images and edge detection results from contact experiments; conformal contact versus modulus of hydrogels; force–displacement curves of hydrogel versus BBN; surface topographies of acrylic surface before and after soil deposition; optical images of elastomers after cleaning; optical images from cleaning experiments with hydrogels (PDF)

■ AUTHOR INFORMATION

Corresponding Author

*E-mail: edwin.chan@nist.gov.

ORCID

Teresa T. Duncan: 0000-0001-7613-0272

Edwin P. Chan: 0000-0003-4832-6299

Funding

T.T.D. acknowledges financial support from the National Research Council (NRC) postdoctoral fellowship program.

Notes

The authors declare no competing financial interest.

■ ACKNOWLEDGMENTS

The authors thank Dr. A. Kotula for help with rheology experiments. The authors also thank Dr. S. Orski and Dr. J. Sarapas for advice provided for the preparation of BBNs. The equipment and instruments or materials are identified in the paper to adequately specify the experimental details. Such identification does not imply recommendation by National Institute of Standards and Technology, nor does it imply the materials are necessarily the best available for the purpose.

■ REFERENCES

- (1) Bietsch, A.; Michel, B. Conformal Contact and Pattern Stability of Stamps Used for Soft Lithography. *J. Appl. Phys.* **2000**, *88* (7), 4310–4318.
- (2) Qin, D.; Xia, Y.; Whitesides, G. M. Soft Lithography for Micro- and Nanoscale Patterning. *Nat. Protoc.* **2010**, *5* (3), 491–502.
- (3) Qiu, Y.; Park, K. Environment-Sensitive Hydrogels for Drug Delivery. *Adv. Drug Delivery Rev.* **2001**, *53*, 321–339.
- (4) Rim, Y. S.; Bae, S. H.; Chen, H.; Yang, J. L.; Kim, J.; Andrews, A. M.; Weiss, P. S.; Yang, Y.; Tseng, H. R. Printable Ultrathin Metal Oxide Semiconductor-Based Conformal Biosensors. *ACS Nano* **2015**, *9* (12), 12174–12181.
- (5) Wainwright, D. K.; Lauder, G. V.; Weaver, J. C. Imaging Biological Surface Topography in Situ and in Vivo. *Methods Ecol. Evol.* **2017**, *8* (11), 1626–1638.
- (6) Liu, L.; Etienne, M.; Walcarius, A. Scanning Gel Electrochemical Microscopy for Topography and Electrochemical Imaging. *Anal. Chem.* **2018**, *90* (15), 8889–8895.
- (7) Persson, B. N. J.; Albohr, O.; Tartaglino, U.; Volokitin, A. I.; Tosatti, E. On the Nature of Surface Roughness with Application to Contact Mechanics, Sealing, Rubber Friction and Adhesion. *J. Phys.: Condens. Matter* **2005**, *17* (1), R1–R62.
- (8) King, D. R.; Bartlett, M. D.; Gilman, C. A.; Irschick, D. J.; Crosby, A. J. Creating Gecko-like Adhesives for “Real World” Surfaces. *Adv. Mater.* **2014**, *26* (25), 4345–4351.
- (9) Fischer, S. C. L.; Arzt, E.; Hensel, R. Composite Pillars with a Tunable Interface for Adhesion to Rough Substrates. *ACS Appl. Mater. Interfaces* **2017**, *9* (1), 1036–1044.
- (10) Warda, J.; Brückle, I.; Bezúr, A.; Kushel, D. Analysis of Agarose, Carbopol, and Laponite Gel Poulitces in Paper Conservation. *J. Am. Inst. Conserv.* **2007**, *46* (3), 263–279.
- (11) Mazza, C.; Micheli, L.; Carbone, M.; Basoli, F.; Cervelli, E.; Iannuccelli, S.; Sotgiu, S.; Palleschi, A. Gellan Hydrogel as a Powerful Tool in Paper Cleaning Process: A Detailed Study. *J. Colloid Interface Sci.* **2014**, *416*, 205–211.
- (12) Duncan, T.; Berrie, B.; Weiss, R. Soft, Peelable Organogels from Partially Hydrolyzed Poly(Vinyl Acetate) and Benzene-1,4-Diboronic Acid: Applications to Clean Works of Art. *ACS Appl. Mater. Interfaces* **2017**, *9* (33), 28069–28078.
- (13) Khandekar, N. A Survey of the Conservation Literature Relating to the Development of Aqueous Gel Cleaning on Painted and Varnished Surfaces. *Rev. Conserv.* **2000**, No. 1, 10–20.
- (14) Doherty, B.; Presciutti, F.; Sgamellotti, A.; Brunetti, B. G.; Miliani, C. Monitoring of Optimized SERS Active Gel Substrates for Painting and Paper Substrates by Unilateral NMR Profilometry. *J. Raman Spectrosc.* **2014**, *45* (11–12), 1153–1159.
- (15) Amato, F.; Micciche, C.; Cannas, M.; Gelardi, F. M.; Pignataro, B.; Li Vigni, M.; Agnello, S. Ag Nanoparticles Agargel Nanocomposites for SERS Detection of Cultural Heritage Interest Pigments. *Eur. Phys. J. Plus* **2018**, *133* (2), 74.
- (16) Wolbers, R. *Cleaning Painted Surfaces: Aqueous Methods*; Archetype Publications: London, 2000.
- (17) Carretti, E.; Bonini, M.; Dei, L.; Berrie, B. H.; Angelova, L. V.; Baglioni, P.; Weiss, R. G. New Frontiers in Materials Science for Art Conservation: Responsive Gels and Beyond. *Acc. Chem. Res.* **2010**, *43* (6), 751–760.

- (18) Samori, C.; Galletti, P.; Giorgini, L.; Mazzeo, R.; Mazzocchetti, L.; Prati, S.; Scitutto, G.; Volpi, F.; Tagliavini, E. The Green Attitude in Art Conservation: Polyhydroxybutyrate-Based Gels for the Cleaning of Oil Paintings. *ChemistrySelect* **2016**, *1* (15), 4502–4508.
- (19) Galatis, P.; Boyatzis, S.; Theodorakopoulos, C. Removal of a Synthetic Soiling Mixture on Mastic, Shellac & Laropal K80 Coatings Using Two Hydrogels. *E-Preservation Sci.* **2012**, *9*, 72–83.
- (20) Domingues, J. A. L.; Bonelli, N.; Giorgi, R.; Fratini, E.; Gorel, F.; Baglioni, P. Innovative Hydrogels Based on Semi-Interpenetrating p(HEMA)/PVP Networks for the Cleaning of Water-Sensitive Cultural Heritage Artifacts. *Langmuir* **2013**, *29* (8), 2746–2755.
- (21) Duncan, T. T.; Berrie, B. H.; Weiss, R. G. Colloidal Properties of Aqueous Poly(Vinyl Acetate)-Borate Dispersions with Short-Chain Glycol Ethers. *ChemPhysChem* **2016**, *17*, 2535–2544.
- (22) Duncan, T. T.; Berrie, B. H.; Weiss, R. G. A Comparison between Gel and Swab Cleaning: Physical Changes to Delicate Surfaces. In *Gels in the Conservation of Art*; Angelova, L. V., Ormsby, B., Townsend, J. H., Wolbers, R., Eds.; Archetype Publications: London, 2017; pp 250–256.
- (23) Tam, A. C.; Leung, W. P.; Zapka, W.; Ziemlich, W. Laser-Cleaning Techniques for Removal of Surface Particulates. *J. Appl. Phys.* **1992**, *71* (7), 3515–3523.
- (24) Siano, S.; Agresti, J.; Cacciari, I.; Ciofini, D.; Mascaldi, M.; Osticioli, I.; Mencaglia, A. A. Laser Cleaning in Conservation of Stone, Metal, and Painted Artifacts: State of the Art and New Insights on the Use of the Nd:YAG Lasers. *Appl. Phys. A: Mater. Sci. Process.* **2012**, *106* (2), 419–446.
- (25) Nilsen, S. K.; Dahl, I.; Jorgensen, O.; Schneider, T. Micro-Fibre and Ultra-Micro-Fibre Cloths, Their Physical Characteristics, Cleaning Effect, Abrasion on Surfaces, Friction, and Wear Resistance. *Buld. Environ.* **2002**, *37* (12), 1373–1378.
- (26) Izadi, H.; Dogra, N.; Perreault, F.; Schwarz, C.; Simon, S.; Vanderlick, T. K. Removal of Particulate Contamination from Solid Surfaces Using Polymeric Micropillars. *ACS Appl. Mater. Interfaces* **2016**, *8* (26), 16967–16978.
- (27) Chateau, M. E.; Galet, L.; Soudais, Y.; Fages, J. A New Test for Cleaning Efficiency Assessment of Cleaners for Hard Surfaces. *J. Surfactants Deterg.* **2004**, *7* (4), 355–362.
- (28) Klier, J.; Tucker, C. J.; Kalantar, T. H.; Green, D. P. Properties and Applications of Microemulsions. *Adv. Mater.* **2000**, *12* (23), 1751–1757.
- (29) Baglioni, P.; Dei, L.; Carretti, E.; Giorgi, R. Gels for the Conservation of Cultural Heritage. *Langmuir* **2009**, *25* (15), 8373–8374.
- (30) Casoli, A.; Cremonesi, P.; Isca, C.; Groppetti, R.; Pini, S.; Senin, N. Evaluation of the Effect of Cleaning on the Morphological Properties of Ancient Paper Surface. *Cellulose* **2013**, *20* (4), 2027–2043.
- (31) Heddleson, S. S.; Hamann, D. D.; Lineback, D. R. The Dahlquist Criterion: Applicability of a Rheological Criterion to the Loss of Pressure-Sensitive Tack in Flour-Water Dough. *Cereal Chem.* **1993**, *70* (6), 744–748.
- (32) Greenwood, J. A.; Williamson, J. B. P. Contact of Nominally Flat Surfaces. *Proc. R. Soc. London A* **1966**, *295*, 300–319.
- (33) Johnson, K. L.; Greenwood, J. A. An Adhesion Map for the Contact of Elastic Spheres. *J. Colloid Interface Sci.* **1997**, *192* (2), 326–333.
- (34) Creton, C.; Leibler, L. How Does Tack Depend on Time of Contact and Contact Pressure? *J. Polym. Sci., Part B: Polym. Phys.* **1996**, *34* (3), 545–554.
- (35) Persson, B. N. J.; Tosatti, E. The Effect of Surface Roughness on the Adhesion of Elastic Solids. *J. Chem. Phys.* **2001**, *115* (12), 5597–5610.
- (36) Persson, B. N. J.; Albohr, O.; Creton, C.; Peveri, V. Contact Area between a Viscoelastic Solid and a Hard, Randomly Rough, Substrate. *J. Chem. Phys.* **2004**, *120* (18), 8779–8793.
- (37) Pastewka, L.; Robbins, M. O. Contact Between Rough Surfaces and a Criterion for Macroscopic Adhesion. *Proc. Natl. Acad. Sci. U. S. A.* **2014**, *111* (9), 3298–3303.
- (38) Kim, H. C.; Russell, T. P. Contact of Elastic Solids with Rough Surfaces. *J. Polym. Sci., Part B: Polym. Phys.* **2001**, *39* (16), 1848–1854.
- (39) Lorenz, B.; Krick, B. A.; Mulakaluri, N.; Smolyakova, M.; Dieluweit, S.; Sawyer, W. G.; Persson, B. N. J. Adhesion: Role of Bulk Viscoelasticity and Surface Roughness. *J. Phys.: Condens. Matter* **2013**, *25* (22), 225004.
- (40) Daniel, W. F. M.; Burdyńska, J.; Vatankhah-Varnoosfaderani, M.; Matyjaszewski, K.; Paturej, J.; Rubinstein, M.; Dobrynin, A. V.; Sheiko, S. S. Solvent-Free, Supersoft and Superelastic Bottlebrush Melts and Networks. *Nat. Mater.* **2016**, *15* (2), 183–189.
- (41) Abbasi, M.; Faust, L.; Wilhelm, M. Comb and Bottlebrush Polymers with Superior Rheological and Mechanical Properties. *Adv. Mater.* **2019**, *31* (26), 1806484.
- (42) Vatankhah-Varnoosfaderani, M.; Daniel, W. F. M.; Everhart, M. H.; Pandya, A. A.; Liang, H.; Matyjaszewski, K.; Dobrynin, A. V.; Sheiko, S. S. Mimicking Biological Stress-Strain Behaviour with Synthetic Elastomers. *Nature* **2017**, *549* (7673), 497–501.
- (43) Sarapas, J. M.; Chan, E. P.; Rettner, E. M.; Beers, K. L. Compressing and Swelling to Study the Structure of Extremely Soft Bottlebrush Networks Prepared by ROMP. *Macromolecules* **2018**, *51* (6), 2359–2366.
- (44) Shull, K. R.; Ahn, D.; Chen, W.-L.; Flanigan, C. M.; Crosby, A. J. Axisymmetric Adhesion Tests of Soft Materials. *Macromol. Chem. Phys.* **1998**, *199*, 489–511.
- (45) Crosby, A. J.; Shull, K. R.; Lakrout, H.; Creton, C. Deformation and Failure Modes of Adhesively Bonded Elastic Layers. *J. Appl. Phys.* **2000**, *88* (5), 2956–2966.
- (46) Schneider, C. A.; Rasband, W. S.; Eliceiri, K. W. NIH Image to ImageJ: 25 Years of Image Analysis. *Nat. Methods* **2012**, *9*, 671–675.
- (47) Gibara, T. Canny Edge Detector, 2013.
- (48) Ormsby, B.; Soldano, A.; Keefe, M. H.; Phenix, A.; Learner, T. An Empirical Evaluation of a Range of Cleaning Agents for Removing Dirt from Artists' Acrylic Emulsion Paints Removing. *AIC Paint. Spec. Gr. Postprints* **2010**, *23*, 1–11.
- (49) Bonelli, N.; Poggi, G.; Chelazzi, D.; Giorgi, R.; Baglioni, P. Poly(Vinyl Alcohol)/Poly(Vinyl Pyrrolidone) Hydrogels for the Cleaning of Art. *J. Colloid Interface Sci.* **2019**, *536*, 339–348.
- (50) Johnson, K. L.; Greenwood, J. A.; Higginson, J. G. The Contact of Elastic Regular Wavy Surfaces. *Int. J. Mech. Sci.* **1985**, *27* (6), 383–396.
- (51) Sullivan, M. R.; Duncan, T. T.; Berrie, B. H.; Weiss, R. G. Rigid Polysaccharide Gels for Paper Conservation: A Residue Study. In *Gels in the Conservation of Art*; Angelova, L. V., Ormsby, B., Townsend, J. H., Wolbers, R., Eds.; Archetype Publications: London, 2017; pp 42–50.
- (52) Hu, Y.; Chan, E. P.; Vlassak, J. J.; Suo, Z. Poroelastic Relaxation Indentation of Thin Layers of Gels. *J. Appl. Phys.* **2011**, *110* (8), 086103.
- (53) Murray, A.; Contreras de Berenfeld, C.; Chang, S. Y. S.; Jablonski, E.; Klein, T.; Riggs, M. C.; Robertson, E. C.; Tse, W. M. A. The Condition and Cleaning of Acrylic Emulsion Paintings. *Mater. Res. Soc. Symp. Proc.* **2002**, *712*, 83–90.
- (54) Sutherland, K. Measurements of Solvent Cleaning Effects on Oil Paintings. *J. Am. Inst. Conserv.* **2006**, *45*, 211–226.
- (55) Ina, M.; Cao, Z.; Vatankhah-Varnoosfaderani, M.; Everhart, M. H.; Daniel, W. F. M.; Dobrynin, A. V.; Sheiko, S. S. From Adhesion to Wetting: Contact Mechanics at the Surfaces of Super-Soft Brush-like Elastomers. *ACS Macro Lett.* **2017**, *6* (8), 854–858.
- (56) De Sá, M. H.; Ferreira, J. L.; Melo, M. J.; Ramos, A. M. An AFM Contribution to the Understanding of Surface Effects Caused by Ageing and Cleaning on Acrylic Glass. The Shadows by Lourdes Castro, a Case Study. *Surf. Interface Anal.* **2011**, *43* (8), 1165–1170.
- (57) Dies, L.; Restagno, F.; Weil, R.; Léger, L.; Poulard, C. Role of Adhesion between Asperities in the Formation of Elastic Solid/Solid Contacts. *Eur. Phys. J. E: Soft Matter Biol. Phys.* **2015**, *38* (12), 1–8.
- (58) Davis, C. S.; Crosby, A. J. Mechanics of Wrinkled Surface Adhesion. *Soft Matter* **2011**, *7* (11), 5373–5381.